Karttunen, Anssi; von Hertzen, Raimo; Reddy, Junthula; Romanoff, Jani

Exact elasticity-based finite element for circular plates

Published in:
Computers and Structures

DOI:
10.1016/j.compstruc.2016.11.013

Published: 01/01/2017

Document Version
Peer-reviewed accepted author manuscript, also known as Final accepted manuscript or Post-print

Exact elasticity-based finite element for circular plates

Anssi T. Karttunen[a,b,*], Raimo von Hertzen[a], J.N. Reddy[b], Jani Romanoff[a]

[a] *Aalto University, Department of Mechanical Engineering, FI-00076 Aalto, Finland*
[b] *Texas A&M University, Department of Mechanical Engineering, College Station, TX 77843-3123, USA*

Abstract

In this paper, a general elasticity solution for the axisymmetric bending of a linearly elastic annular plate is used to derive an exact finite element for such a plate. We start by formulating an interior plate problem by employing Saint Venant's principle so that edge effects do not appear in the plate. Then the elasticity solution to the formulated interior problem is presented in terms of mid-surface variables so that it takes a form similar to conventional engineering plate theories. By using the mid-surface variables, the exact finite element is developed both by force- and energy-based approaches. The central, non-standard feature of the interior solution, and the finite element based on it, is that the interior stresses of the plate act as surface tractions on the plate edges and contribute to the total potential energy of the plate. Finally, analytical and numerical examples are presented using the elasticity solution and the derived finite element.

Keywords: Interior plate, Saint Venant's principle, Clapeyron's theorem, Betti's theorem, finite element, numerical examples

1. Introduction

It is relatively easy to derive general closed-form solutions for the axisymmetric bending of linearly elastic circular Kirchhoff, Mindlin and Levinson plates [1–3]. Furthermore, the analytical solutions may be used to develop exact, locking-free plate finite elements [4–6]. Closed-form elasticity solutions that relax the kinematic and constitutive assumptions of the aforementioned conventional plate theories, however, are not that well-known; the only solution found in standard textbooks is the one for a uniformly loaded simply-supported solid circular plate [7, 8]. Thus, it comes as no surprise that exact finite elements for the axisymmetric bending of circular plates founded on closed-form elasticity solutions do not exist. In this paper, we develop such an element by using a suitable general elasticity solution.

The exact elasticity solution for the uniformly loaded simply-supported circular plate [7] is in fact an *interior* solution that excludes all edge effects by virtue of Saint Venant's principle. When a *full* solution is of interest, the most general state of stress within a linearly elastic, isotropic, homogeneous plate can be decomposed into three parts: (1) interior state, (2) shear state, and (3) Papkovich–Fadle state [9–11]. Detailed, general 3D elasticity solutions for plates which account for all three states have been given by several authors [12–17]. The shear and Papkovich–Fadle

Recompiled, unedited accepted manuscript. **Cite as**: *Comput. Struct.* 2017;182:219–226 doi link
*Corresponding author. anssi.karttunen@iki.fi

states are indeed predominantly related to edge effects, whereas the interior state represents the conventional "plate theory part" [9]. We use the general interior solution of Piltner [16], obtained by using displacement potentials, to derive an exact finite element for the axisymmetric bending of circular plates. General interior elasticity solutions derived using the Airy stress function have been recently used to develop finite elements for plane beams in a likewise manner [18, 19].

The distinction between the three different stress states is highly important due to the fact that if our plate consists solely of the interior state, the interior stresses of the plate act as surface tractions on the lateral edges of the plate and, thus, they contribute significantly to the total potential energy of the plate. It is commonplace not to account for this property in energy-based treatments of plate theories founded exclusively on interior behavior. Therefore, the energy-based formulation of the plate finite element to be presented herein is fundamentally different from the conventional practices because we take the work due to the interior stresses on the plate edges properly into account. Although the present study is limited to linearly elastic, isotropic, homogeneous plates that undergo small deformations, the employed interior methodology is expected to find wider application in the study of engineering plate theories.

The remainder of this paper is organized in the following way. In Section 2, an interior problem is formulated for a circular plate and the implications of the interior definition are discussed. In Section 3, the general elasticity solution to the formulated problem is studied. Using mid-surface variables formed from the solution, an exact axisymmetric annular plate finite element is formulated in Section 4 both by force- and energy-based methods. A variety of analytical and numerical examples are presented in Section 5. Finally, conclusions are drawn in Section 6.

2. Interior problem formulation

2.1. Boundary conditions

A linearly elastic, isotropic, homogeneous annular plate under a rotationally symmetric transverse load p is shown in Fig. 1. The thickness of the plate is h and the outer and inner radii of the plate are a and b, respectively. The stress boundary conditions on the upper and lower faces of the plate read

$$\sigma_z(r,-h/2)=-p, \quad \sigma_z(r,h/2)=0, \quad \tau_{rz}(r,\pm h/2)=0. \tag{1}$$

The boundary conditions are introduced in a *strong* (pointwise) sense for the upper and lower faces. On the inner and outer lateral edges of the plate the tractions are specified through stress resultants as suggested by Fig. 1 and, thus, the boundary conditions on the lateral edges are imposed only in a *weak* sense [8]. The stress resultants per unit length are calculated from the equations

$$M_r=\int_{-h/2}^{h/2}\sigma_r z dz,\ M_\theta=\int_{-h/2}^{h/2}\sigma_\theta z dz,\ Q_r=\int_{-h/2}^{h/2}\tau_{rz}dz, \tag{2}$$

where $M_r(r)$ and $Q_r(r)$ are the radial bending moment and shear force, respectively, and $M_\theta(r)$ is the tangential bending moment. The positive directions of the radial stress resultants are given in Fig. 1.

The replacement of the strong stress boundary conditions along the plate edges by the statically equivalent weak boundary conditions (stress resultants) implies that all detailed, exponentially decaying edge effects of the plate are eliminated by virtue of Saint Venant's principle and only the interior solution of the plate is under consideration. The general homogeneous solution by Piltner [16] to the formulated interior plate problem for stress-free faces will be studied in Section 3. A uniformly distributed load will be added as the particular contribution to the solution.

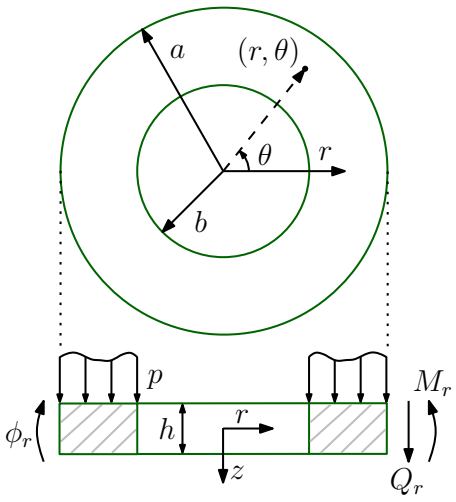

Figure 1: Axisymmetric annular interior plate under a rotationally symmetric transverse load p on the upper face. The positive directions of the stress resultants and rotation ϕ_r on the outer edge are shown.

2.2. Boundary layer and implications of the interior definition

Let us consider the solid circular plate with a boundary layer shown in Fig. 2. If pointwise boundary conditions were to be imposed on the outer edge of the boundary layer at $r = a'$, the detailed distributions of the resulting stresses would bring about edge effects which decay exponentially towards the interior of the plate. As a rule of thumb in isotropic cases, the boundary layer is as thick as the plate itself, that is, the thinner the plate is, the weaker the edge effects are. Studying a plate which consists only of an interior part means that the boundary layer has been removed. This amounts to fully-developed interior stresses being active all-over the plate at hand, including the lateral plate edge, where they act as surface tractions. In the case of an annular plate, an analogous discussion may be extended to the inner boundary region.

The key feature of the interior plate definition is that the interior stresses acting as surface tractions contribute to the total potential energy of the plate which reads

$$\Pi = U - W_p - W_s \tag{3}$$

where the strain energy for an annular plate is

$$U = \pi \int_b^a \int_{-h/2}^{h/2} r(\sigma_r \epsilon_r + \sigma_\theta \epsilon_\theta + \sigma_z \epsilon_z + \tau_{rz}\gamma_{rz}) dz dr \tag{4}$$

and the external work due to a uniformly distributed load $p = p_0$, which is of interest to us in the following sections, is given by

$$W_p = 2\pi \int_b^a r p_0 U_z(r, -h/2) dr. \tag{5}$$

The work by the surface tractions due to the interior stresses on the outer and inner lateral edges of the interior plate is given by

$$W_s = 2\pi a \int_{-h/2}^{h/2} [\sigma_r U_r + \tau_{rz} U_z](a, z) dz - 2\pi b \int_{-h/2}^{h/2} [\sigma_r U_r + \tau_{rz} U_z](b, z) dz. \tag{6}$$

where $U_r(r, z)$ and $U_z(r, z)$ are the displacements in the directions of r and z, respectively.

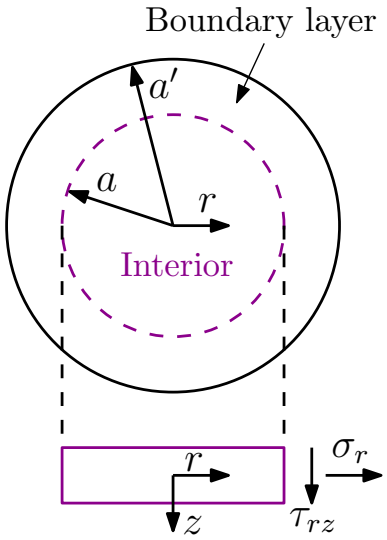

Figure 2: Solid circular plate consisting of an interior part and a boundary layer. When only the interior plate is studied, stresses σ_r and τ_{rz} do work on the plate edge.

3. General interior elasticity solution

3.1. Homogeneous solution

Starting from Piltner's [16] solution for a rectangular plate, the general interior solution for a linearly elastic, isotropic, homogeneous circular plate with stress-free upper and lower faces (homogeneous case) can be written as

$$2G \cdot U_r^h = -z\frac{\partial \Psi}{\partial r} - \frac{1}{4(1-\nu)}\left[h^2 z - 2(2-\nu)\frac{z^3}{3}\right]\frac{\partial}{\partial r}\nabla^2\Psi, \tag{7}$$

$$2G \cdot U_z^h = \Psi + \frac{\nu z^2}{2(1-\nu)}\nabla^2\Psi, \tag{8}$$

where G and ν are the shear modulus and Poisson ratio, respectively. Furthermore, we have

$$\nabla^2 = \frac{1}{r}\frac{\partial}{\partial r}\left(r\frac{\partial}{\partial r}\right) \quad \text{and} \quad \nabla^4\Psi = 0. \tag{9}$$

The general solution to Eq. $(9)_2$ is

$$\Psi = c_1 + c_2 r^2 + c_3 \ln r + c_4 r^2 \ln r. \tag{10}$$

We see that every term in the biharmonic function Ψ is multiplied by an arbitrary constant c_i $(i = 1, 2, 3, 4)$. In practical engineering problems, these constants are determined from conditions that imitate actual, pointwise boundary conditions. This is the standard practice also in the context of 2D linear elasticity when interior plane beam problems are studied using Airy stress functions, see Ref. [7]. If a proper boundary layer for the plate is desired, elasticity solutions that deal with Papkovich-Fadle functions may be used as the starting point, see Ref. [16].

3.2. Particular solution for uniformly distributed load

We consider a particular solution for a uniformly distributed load $p = p_0$ acting on the upper face of the plate (see Fig. 1). The solution for such a load is [16]

$$2G \cdot U_r^p = \frac{p_0 r}{4h^3}\left[(2-\nu)(4z^3 - 3h^2 z) - 3(1-\nu)r^2 z + \frac{2\nu h^3}{1+\nu}\right], \tag{11}$$

$$2G \cdot U_z^p = \frac{p_0}{16h^3}\Bigg[24\nu r^2 z^2 - 8(1+\nu)z^4 + 12h^2(1+\nu)z^2 + 3(1-\nu)r^4 - 6\nu h^2 r^2 - \frac{8h^3 z}{1+\nu}\Bigg]. \tag{12}$$

Solutions for different distributed loads may be developed by following the work of Piltner [16].

3.3. Displacement field, strains and stresses

The total displacements are given by

$$U_r(r,z) = U_r^h(r,z) + U_r^p(r,z), \tag{13}$$

$$U_z(r,z) = U_z^h(r,z) + U_z^p(r,z), \tag{14}$$

In order to present displacements (13) and (14) in terms of mid-surface variables like in the case of conventional plate theories, we define

$$u_r(r) \equiv U_r(r,0) = \frac{p_0 \nu r}{2E}, \tag{15}$$

$$u_z(r) \equiv U_z(r,0) = \frac{1}{2G}\Psi - \frac{3p_0 r^2(1+\nu)}{16Eh^3}\left[r^2(\nu-1) + 2\nu h^2\right], \tag{16}$$

$$\phi_r(r) \equiv \frac{\partial U_r}{\partial z}(r,0) = -\frac{1}{2G}\frac{\partial}{\partial r}\left[\Psi + \frac{h^2}{4(1-\nu)}\nabla^2\Psi\right] + \frac{3p_0 r(1+\nu)}{4Eh^3}\left[h^2(\nu-2) + (\nu-1)r^2\right], \tag{17}$$

where $E = 2G(1+\nu)$ is the Young's modulus, u_r and u_z are the radial displacement and transverse deflection on the mid-surface, respectively, and ϕ_r is the rotation of the normal of the mid-surface. It can be shown that

$$\phi_r = -\frac{\partial}{\partial r}\left[u_z + \frac{h^2}{4(1-\nu)}\nabla^2 u_z\right]. \tag{18}$$

By using the mid-surface variables, displacements (13) and (14) can be written as

$$U_r = u_r + z\phi_r - \frac{4z^3}{3h^2}\left(\phi_r + \frac{\partial u_z}{\partial r}\right) - \frac{\nu z^3}{6(1-\nu)}\frac{\partial}{\partial r}\nabla^2 u_z, \tag{19}$$

$$U_z = u_z + \frac{\nu z^2}{2(1-\nu)}\nabla^2 u_z - \frac{p_0 z}{2Eh}\left[\frac{h^3 + z^3(1+\nu)^2}{h^2} - \frac{3z(1+\nu)}{2(1-\nu)}\right]. \tag{20}$$

It is interesting to note that if we neglect the distributed load and the Poisson effect ($p_0 = \nu = 0$) in Eqs. (19) and (20), the displacement field is exactly of the same form as that for the Levinson and Reddy plate theories [2, 6]. Furthermore, when the third-order contribution z^3 is eliminated, the kinematic description for the Mindlin plate theory is obtained. Finally, in the limit $h \to 0$,

Eq. (18) gives $\phi_r = -\partial u_z/\partial r$, which brings us to the Kirchhoff plate theory. In fact, Eqs. (16) and (17) with Eq. (10) are the general solution for the axisymmetric bending of circular Levinson and Mindlin plates (shear coefficient $\kappa = 2/3$) subjected to a uniform distributed load.

The strains of the elasticity-based circular plate are calculated from

$$\epsilon_r = \frac{\partial U_r}{\partial r},\ \epsilon_\theta = \frac{U_r}{r},\ \epsilon_z = \frac{\partial U_z}{\partial z},\ \gamma_{rz} = \frac{\partial U_r}{\partial z} + \frac{\partial U_z}{\partial r}. \tag{21}$$

The stresses are given by

$$\begin{aligned} \sigma_r &= (2G+\lambda)\epsilon_r + \lambda\epsilon_\theta + \lambda\epsilon_z, \\ \sigma_\theta &= \lambda\epsilon_r + (2G+\lambda)\epsilon_\theta + \lambda\epsilon_z, \\ \sigma_z &= \lambda\epsilon_r + \lambda\epsilon_\theta + (2G+\lambda)\epsilon_z, \\ \tau_{rz} &= G\gamma_{rz}, \end{aligned} \tag{22}$$

where

$$\lambda = \frac{E\nu}{(1+\nu)(1-2\nu)}. \tag{23}$$

The following stress equations are needed for the finite element developments. We calculate the stress resultants (2) using the stresses (22) and the general solution. Then, we write the constant coefficients c_2, c_3 and c_4 in terms of the stress resultants and substitute them back into (22) to obtain

$$\sigma_r = \frac{12M_r z}{h^3} - \frac{z(3h^2-20z^2)}{10h^3 r}\left[2p_0 r - (\nu-2)Q_r\right], \tag{24}$$

$$\sigma_\theta = \frac{12M_\theta z}{h^3} - \frac{z(3h^2-20z^2)}{10h^3 r}\left[p_0\nu r + (\nu-2)Q_r\right], \tag{25}$$

$$\sigma_z = -\frac{p_0}{2h^3}(h+z)(h-2z)^2, \tag{26}$$

$$\tau_{rz} = \frac{3Q_r}{2h^3}(h^2-4z^2)\ . \tag{27}$$

Finally, by integrating the 3D stress equilibrium equations given in the cylindrical coordinate system with respect to the thickness coordinate z, we obtain (for the derivation, see Ref. [20])

$$\frac{\partial}{\partial r}(rM_r) - M_\theta = rQ_r, \tag{28}$$

$$\frac{\partial}{\partial r}(rQ_r) = -rp_0. \tag{29}$$

In summary, the foregoing general interior solution constitutes a plate theory of the conventional form that includes the Kirchhoff, Mindlin and Levinson theories as special cases.

3.4. Remarks on energetical aspects

Let us briefly consider some energy-related issues.

- If the plate equilibrium equations (28) and (29) were to be derived using a variational method, for example, the principle of virtual displacements, the inclusion of the virtual work δW_s [cf. Eq. (6)] to the derivation would lead to *interior boundary conditions* that eliminate artificial edge effects, or equivalently, higher-order stress resultants from the plate. For details, see the recent variational interior formulation of the Levinson theory for circular plates [6].

- According to Clapeyron's theorem, the strain energy stored in an elastic body is equal to one-half of the work done by the surface tractions and body forces if they were to move (slowly) through their respective displacements from an unstressed state to the state of equilibrium [21]. In the present case, Clapeyron's theorem leads to

$$2U - W_p - W_s = 0. \tag{30}$$

- Say we have two biharmonic solution functions $\Psi^{(1)}$ and $\Psi^{(2)}$ [cf. Eq. (10)] with different arbitrary constants $c_i^{(1)}$ and $c_i^{(2)}$ $(i = 1, 2, 3, 4)$, respectively. Then according to Betti's reciprocal theorem and Eq. (6), we have (for $p = 0$)

$$\begin{aligned} &2\pi a \int_{-h/2}^{h/2} [\sigma_r^{(1)} U_r^{(2)} + \tau_{rz}^{(1)} U_z^{(2)}](a, z) dz - 2\pi b \int_{-h/2}^{h/2} [\sigma_r^{(1)} U_r^{(2)} + \tau_{rz}^{(1)} U_z^{(2)}](b, z) dz \\ &= 2\pi a \int_{-h/2}^{h/2} [\sigma_r^{(2)} U_r^{(1)} + \tau_{rz}^{(2)} U_z^{(1)}](a, z) dz - 2\pi b \int_{-h/2}^{h/2} [\sigma_r^{(2)} U_r^{(1)} + \tau_{rz}^{(2)} U_z^{(1)}](b, z) dz. \end{aligned} \tag{31}$$

It is easy to verify, by the aid of a symbolic computation tool such as Mathematica, that Clapeyron's (30) and Betti's (31) theorems are satisfied by the general interior solution given by Eqs. (19) and (20). While Clapeyron's theorem confirms the validity of the interior formulation discussed in Section 2 in a simple manner, Betti's reciprocal theorem serves as a vehicle for discussion in the next section, where the stiffness matrix of the plate element based on the elasticity solution turns out to be asymmetric.

4. Exact annular interior plate finite element

4.1. Displacements in terms of FE degrees of freedom

The general interior elasticity solution can be used as the basis for the derivation of an exact annular plate finite element (FE). The force-based derivation to be presented below is similar to that presented by Reddy et al. [4] for an annular Mindlin plate (except for the distributed load p_0 added here). As the point of departure in terms of methodology, we develop the plate element also by the principle of minimum total potential energy. Fig. 3 presents the setting according to which the finite element is developed. Each node in Fig. 3 has two degrees of freedom, namely, transverse displacement $u_{z,i}$ and rotation $\phi_{r,i}$ $(i = 1, 2)$. Using Eqs. (16) and (17), we define the FE degrees of freedom as

$$\begin{aligned} u_{z,1} &= u_z(b), \qquad & u_{z,2} &= u_z(a), \\ \phi_{r,1} &= \phi_r(b), \qquad & \phi_{r,2} &= \phi_r(a). \end{aligned} \tag{32}$$

In matrix form we have

$$\mathbf{u} = \mathbf{H}\mathbf{c} + \mathbf{u_p}, \tag{33}$$

where

$$\mathbf{c} = \{c_1 \quad c_2 \quad c_3 \quad c_4\}^{\mathrm{T}}, \tag{34}$$

$$\mathbf{u} = \{u_{z,1} \quad \phi_{r,1} \quad u_{z,2} \quad \phi_{r,2}\}^{\mathrm{T}}, \tag{35}$$

$$\mathbf{u_p} = \frac{3p_0}{32Gh^3} \begin{Bmatrix} -b^4(\nu - 1) - 2b^2h^2\nu \\ 4b\left[h^2(\nu - 2) + b^2(\nu - 1)\right] \\ -a^4(\nu - 1) - 2a^2h^2\nu \\ 4a\left[h^2(\nu - 2) + a^2(\nu - 1)\right] \end{Bmatrix}, \tag{36}$$

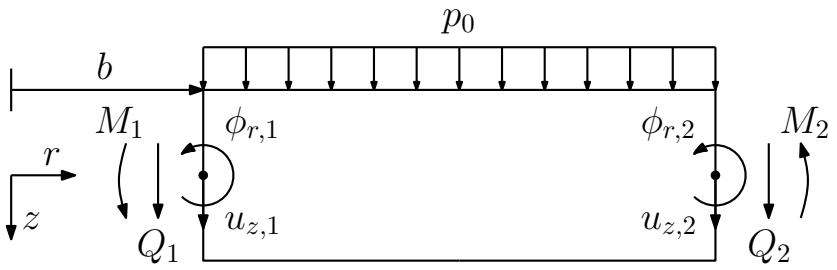

Figure 3: Set-up according to which the exact annular circular plate finite element is developed.

$$\mathbf{H} = \frac{1}{2G}\begin{bmatrix} 1 & b^2 & \ln b & b^2 \ln b \\ 0 & -2b & -\frac{1}{b} & -b(1+2\ln b) + \frac{h^2}{b(\nu-1)} \\ 1 & a^2 & \ln a & a^2 \ln a \\ 0 & -2a & -\frac{1}{a} & -a(1+2\ln a) + \frac{h^2}{a(\nu-1)} \end{bmatrix}. \tag{37}$$

The constants coefficients c_i $(i = 1, 2, 3, 4)$ are obtained in terms of the FE degrees of freedom by

$$\mathbf{c} = \mathbf{H}^{-1}(\mathbf{u} - \mathbf{u_p}). \tag{38}$$

Then the total displacements (13) and (14) in terms of the FE degrees of freedom may be written as

$$\mathbf{U} = \mathbf{L}\mathbf{c} + \mathbf{U_p}, \tag{39}$$

where

$$\mathbf{U} = \{U_r \quad U_z\}^{\mathrm{T}}, \tag{40}$$

$$\mathbf{L} = \frac{1}{2G}\begin{bmatrix} 0 & -2rz & -\frac{z}{r} & \frac{z\left[3h^2+2z^2(\nu-2)\right]}{3r(\nu-1)} - rz(1+2\ln r) \\ 1 & r^2 - \frac{2\nu z^2}{\nu-1} & \ln r & r^2 \ln r - \frac{2\nu z^2}{\nu-1}(1+\ln r) \end{bmatrix}, \tag{41}$$

$$\mathbf{U_p} = \frac{p_0}{32Gh^3}\begin{Bmatrix} 12r^3 z(\nu-1) + 4rz(\nu-2)(3h^2-4z^2) + \frac{8\nu h^3 r}{1+\nu} \\ 4z^2(1+\nu)(3h^2-2z^2) - 6\nu r^2(h^2-4z^2) - 3r^4(\nu-1) - \frac{8h^3 z}{1+\nu} \end{Bmatrix}. \tag{42}$$

We see that once the nodal displacements are known, the total displacement field is obtained by substituting them into Eq. (39), after which the calculation of the interior strains and stresses is straightforward. We note that the shape functions for $\mathbf{U}$ are given by $\mathbf{L}\mathbf{H}^{-1}$. However, the following derivations of the finite element equations do not require the use of the shape functions in the conventional manner.

4.2. Finite element equations

4.2.1. Force-based approach

The nodal forces for the finite element are

$$\begin{aligned} Q_1 &= -2\pi(rQ_r)_{r=b}\,, & Q_2 &= 2\pi(rQ_r)_{r=a}\,, \\ M_1 &= -2\pi(rM_r)_{r=b}\,, & M_2 &= 2\pi(rM_r)_{r=a}\,, \end{aligned} \tag{43}$$

or in matrix form

$$\mathbf{f} = \mathbf{G}\mathbf{c} + \mathbf{f_p}, \tag{44}$$

where

$$\mathbf{f} = \{Q_1 \quad M_1 \quad Q_2 \quad M_2\}^{\mathrm{T}}, \tag{45}$$

$$\mathbf{f_p} = p_0\pi \begin{Bmatrix} b^2 \\ \frac{b}{40}\left[4h^2(2+\nu)+5b^2(3+\nu)\right] \\ -a^2 \\ -\frac{a}{40}\left[4h^2(2+\nu)+5a^2(3+\nu)\right] \end{Bmatrix}, \tag{46}$$

$$\mathbf{G} = \pi\frac{D}{G}\begin{bmatrix} 0 & 0 & 0 & 4 \\ 0 & 2b(1+\nu) & \frac{\nu-1}{b} & \Lambda_b - \frac{(8+\nu)h^2}{10b} \\ 0 & 0 & 0 & -4 \\ 0 & -2a(1+\nu) & -\frac{\nu-1}{a} & -\Lambda_a + \frac{(8+\nu)h^2}{10a} \end{bmatrix}, \tag{47}$$

with

$$D = \frac{Eh^3}{12(1-\nu^2)}, \tag{48}$$

$$\Lambda_b = b[(3+\nu) + 2(1+\nu)\ln b], \tag{49}$$

$$\Lambda_a = a[(3+\nu) + 2(1+\nu)\ln a]. \tag{50}$$

By virtue of Eqs. (38) and (44) we arrive at the finite element equations

$$\mathbf{Ku} = \mathbf{f} + \mathbf{p}, \tag{51}$$

where the stiffness matrix is

$$\mathbf{K} = \mathbf{GH}^{-1} \tag{52}$$

and the uniformly distributed load contributes by

$$\mathbf{p} = \mathbf{GH}^{-1}\mathbf{u_p} - \mathbf{f_p}. \tag{53}$$

4.2.2. Energy method

Let us consider the derivation of the finite element equations from the total potential energy given by Eq. (3). The stresses on the plate edges $r = b$ and $r = a$ in Eq. (6) are written as given by Eqs. (24) to (27), where the stress resultants originally defined per unit length are expressed as nodal loads so that

$$\begin{aligned} \frac{W_s}{2\pi} &= a\int_{-h/2}^{h/2}\left\{\frac{12z}{h^3}\frac{(+M_2)}{2\pi a} - \frac{z(3h^2-20z^2)}{10h^3a}\left[2pa-(\nu-2)\frac{(+Q_2)}{2\pi a}\right]\right\}U_r(a,z)dz \\ &- b\int_{-h/2}^{h/2}\left\{\frac{12z}{h^3}\frac{(-M_1)}{2\pi b} - \frac{z(3h^2-20z^2)}{10h^3b}\left[2pb-(\nu-2)\frac{(-Q_1)}{2\pi b}\right]\right\}U_r(b,z)dz \\ &+ a\int_{-h/2}^{h/2}\left[\frac{3}{2h^3}\frac{(+Q_2)}{2\pi a}(h^2-4z^2)\right]U_z(a,z)dz \\ &- b\int_{-h/2}^{h/2}\left[\frac{3}{2h^3}\frac{(-Q_1)}{2\pi b}(h^2-4z^2)\right]U_z(b,z)dz. \end{aligned} \tag{54}$$

Then, by using Eqs. (38) and (39) to calculate the total potential energy (3) and by applying the principle of minimum total potential energy

$$\frac{\partial \Pi}{\partial u_{z,1}} = 0, \ \frac{\partial \Pi}{\partial u_{z,2}} = 0, \ \frac{\partial \Pi}{\partial \phi_{r,1}} = 0, \ \frac{\partial \Pi}{\partial \phi_{r,2}} = 0 \tag{55}$$

we obtain the finite element equations (51). The labourious calculations may be carried out using Mathematica. We see that the work W_s done by the interior stresses is an integral part of the formulation that introduces the nodal forces into the finite element equations (51).

4.2.3. Notes on the derived element

A notable feature of the stiffness matrix (52) is that it is not symmetric. Regardless of the asymmetry, the plate element, which is an alternative representation of the interior elasticity solution discussed in Section 3, does not violate Betti's reciprocal theorem [cf. Eq. (31)]. With regard to Betti's theorem, it is noteworthy that every nodal load in the interior edge work W_s [Eq. (54)] is associated with every nodal degree of freedom. For example, Q_1 is not conjugate only to $u_{z,1}$ in the conventional manner ($Q_1 \cdot u_{z,1}$), but also to all the other degrees of freedom. Finally, we note that in the limit $h \to 0$ we obtain from Eq. (52) the stiffness matrix of the Kirchhoff plate element, which is symmetric.

5. Analytical and numerical case studies

5.1. Solid circular plates under uniform pressure

Let us first consider solid circular plates subjected to a uniformly distributed load using the general solution discussed in Section 3. The displacements are taken to be finite at the centerpoint of the solid plate and, thus, $c_3 = c_4 = 0$ in Eq. (10). The remaining non-zero constants c_1 and c_2 are solved using the boundary conditions

$$\begin{aligned} &r = a: \ u_z = M_r = 0 \quad \text{(simply-supported)}, \\ &r = a: \ u_z = \phi_r = 0 \quad \text{(clamped)}. \end{aligned} \tag{56}$$

Using Eqs. $(2)_1$, (16) and (17), the transverse deflection on the mid-surface of the simply-supported plate becomes

$$u_z = \frac{3p}{80Eh^3}(a^2 - r^2)\big[5r^2(\nu^2 - 1) - 5a^2(\nu - 1)(5 + \nu) + 2h^2(8 + \nu + \nu^2)\big] \tag{57}$$

and for the clamped plate we get

$$u_z = \frac{3p}{16Eh^3}(a^2 - r^2)\big[4h^2(1 + \nu) + (a^2 - r^2)(1 - \nu^2)\big]. \tag{58}$$

The rotation of the normal of the mid-surface is calculated from Eq. (18). The full, exact displacement solutions, which are believed to be novel, are obtained by substituting the mid-surface variables into Eqs. (19) and (20), after which the strains and stresses are obtained from Eqs. (21) and (22), respectively. It is easy to verify that the stresses of the simply-supported plate obtained this way are the same as those in literature obtained via a stress function approach [7]. The solutions for the Mindlin and Levinson plates are found by starting from Eqs. (16) and (17), which are the general solution for the axisymmetric bending of circular Levinson and Mindlin plates.

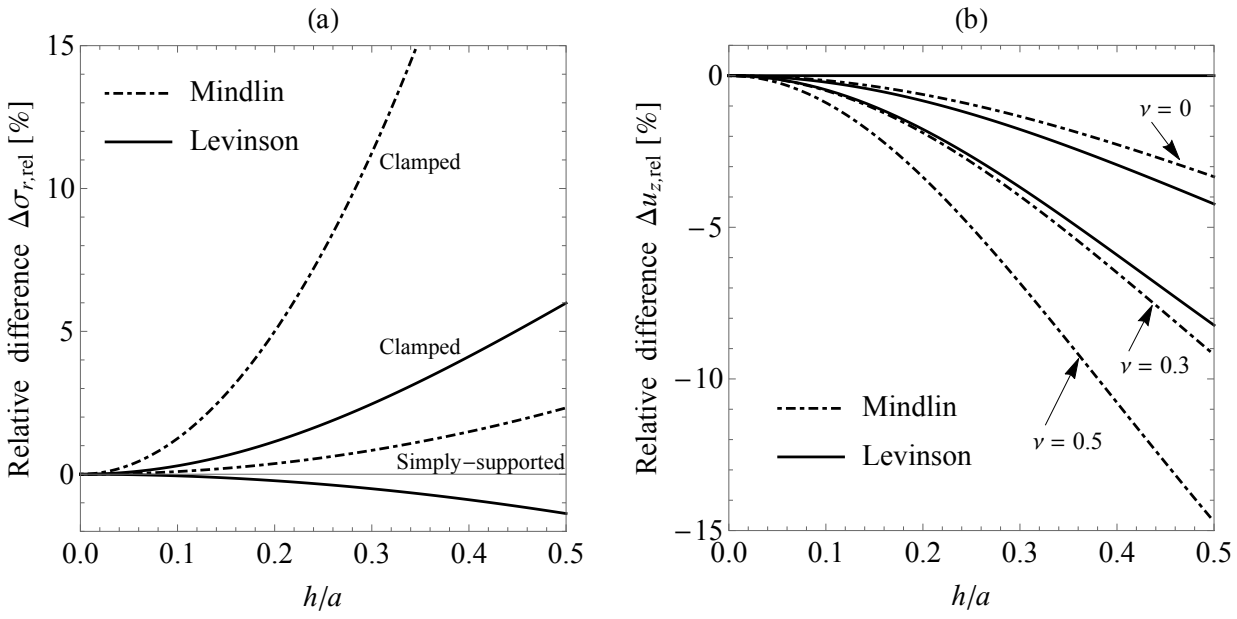

Figure 4: a) Relative differences between the present exact solution and corresponding Mindlin and Levinson solutions in terms of $\sigma_r(0,-h/2)$ for clamped and simply-supported solid circular plates under a uniformly distributed load. b) Relative differences in terms of $u_z(0)$ in the case of a simply-supported plate.

Figure 4(a) displays the relative differences between the present exact interior solution and the Mindlin and Levinson solutions in terms of the radial normal stress $\sigma_r(0,-h/2)$ calculated from

$$\Delta\sigma_{r,\mathrm{rel}} = 100 \times \frac{\sigma_{r,\mathrm{Present}} - \sigma_{r,\mathrm{Levinson/Mindlin}}}{\sigma_{r,\mathrm{Levinson/Mindlin}}} \,. \tag{59}$$

The parameter values for the numerical calculations were taken as $E = 210$ GPa, $\nu = 0.3$, $a = 1$ m, and $p_0 = 1$ MPa. The plate thickness was varied in the calculations. We see from Fig. 4(a) that the Mindlin and Levinson theories give good approximations of the stress for thin and moderately thick plates in the simply-supported case. In the clamped case, the differences between the present exact and approximate solutions grow more rapidly as the $h/a-$ratio increases. Figure 4(b) shows the relative differences in terms of the maximum transverse deflection $u_z(0)$ for two different values of the Poisson ratio in the case of the simply-supported plate. For $\nu = 0$, the Levinson plate gives the same result as the present one. In the clamped case the Mindlin and Levinson theories give the same mid-surface displacements as the present one ($\kappa = 2/3$ for Mindlin).

5.2. Annular circular plates attached to a rigid shaft

Next we consider annular plates attached at their inner edges to a rigid shaft which is subjected to a vertical point load P at its centerpoint. To obtain the exact interior elasticity solution, only one finite element is needed. The boundary conditions for the present case are

$$\begin{aligned} &\phi_{r,1} = u_{z,2} = 0 && \text{(outer edge simply-supported)}, \\ &\phi_{r,1} = \phi_{r,2} = u_{z,2} = 0 && \text{(outer edge clamped)} \end{aligned} \tag{60}$$

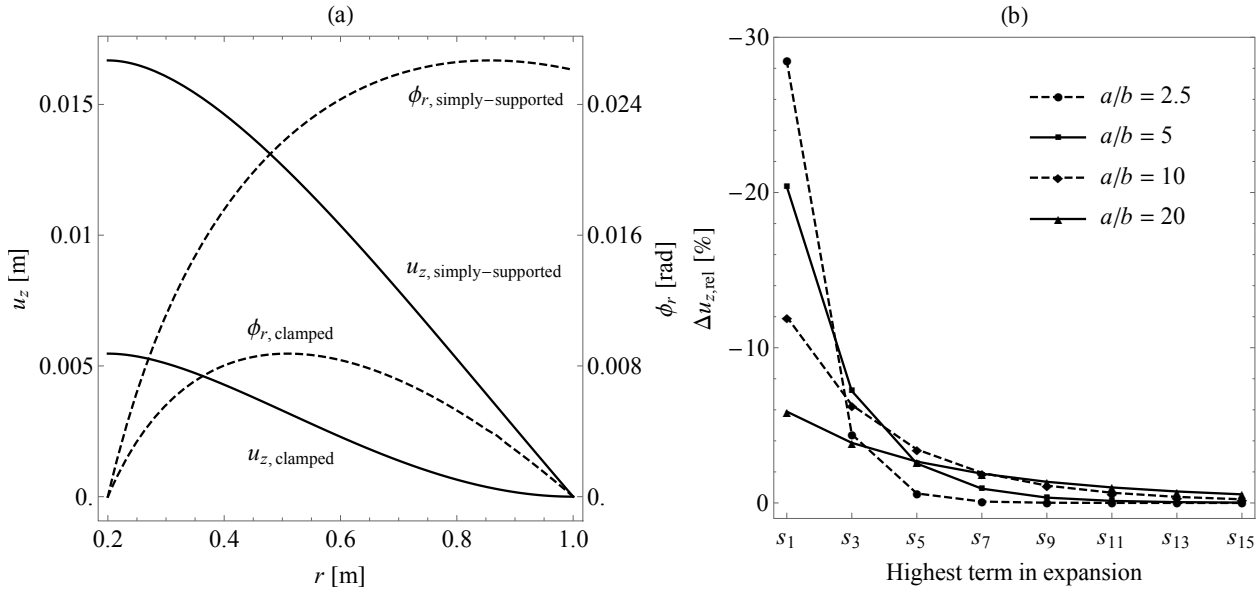

Figure 5: a) Displacements of annular plates with simply-supported and clamped outer edges attached to a rigid point-loaded shaft. b) Relative differences for clamped plates in terms of $u_{z,1}$ with exact solution as reference and the logarithmic terms in Eq. (62) expanded to a varying degree according to Eq. (61).

and $Q_1 = P$. After solving the nodal displacements from Eq. (51), the full displacements are calculated from Eqs. (38) and (39). The mid-surface displacements are shown in Fig. 5(a) for $E = 210$ GPa, $\nu = 0.3$, $h = 0.01$ m, $b = 0.2$ m, $a = 1$ m and $P = 10^4$ N.

The stiffness matrix (52) contains logarithmic terms. However, it is customary to base the derivation of finite elements on (low-order) polynomial shape functions. Thus, it is of interest to expand the logarithmic terms by

$$\ln \alpha = 2 \left[\left(\frac{\alpha - 1}{\alpha + 1} \right)^1 + \frac{1}{3} \left(\frac{\alpha - 1}{\alpha + 1} \right)^3 + \frac{1}{5} \left(\frac{\alpha - 1}{\alpha + 1} \right)^5 + \ldots \right] \quad \text{for} \quad \alpha > 0 \tag{61}$$

to study how many terms in the series are needed to obtain accurate results. To this end, the exact interior transverse deflection in the clamped case at the inner edge of the plate is given by

$$u_{z,1} = \frac{3P}{4\pi} \frac{(1 - \nu^2)}{Eh^3} \left[a^2 - b^2 - \frac{4a^2 b^2}{a^2 - b^2} \ln^2 \left(\frac{a}{b} \right) - \frac{2h^2}{\nu - 1} \ln \left(\frac{a}{b} \right) \right]. \tag{62}$$

Figure 5(b) shows the relative difference in terms of displacement (62) between the exact solution and solutions in which the logarithmic terms have been expanded according to Eq. (61); subscript i of s_i refers to the exponent of the highest term included in the expansion (61). In the calculations the value of the inner radius b was varied. We see that for the lowest order approximation (s_1) the relative difference and the diameter of the shaft increase hand in hand. When additional terms are included in the expansion, the results coalesce and converge smoothly. An interesting trend in the figure is that the smaller the $a/b-$ratio is, the faster the results tend converge as terms are added in the expansion.

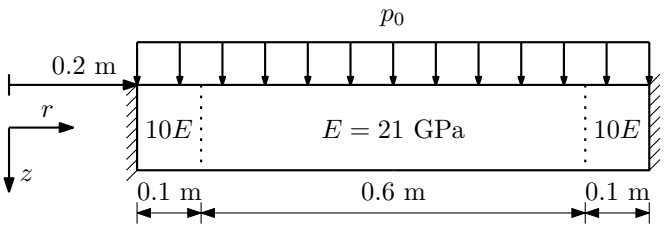

Figure 6: Right-hand side of a clamped-clamped annular circular plate subjected to a uniformly distributed load.

5.3. Clamped-clamped plate with varying properties

Figure 6 shows an annular plate subjected to a uniform load. The edge regions of the plate are notably stiffer than the core of the plate. The plate is modeled by three finite elements. Generally speaking, any discontinuity such as a load, support or change of material properties along the radial direction requires a new element. With clamped-clamped boundary conditions and $\nu = 0.3$, $h = 0.01$ m and $p_0 = 10^5$ Pa, we obtain the mid-surface displacements shown in Fig. 7. The results for a plate with a constant Young's modulus are also given. It should be noted that the *interior* finite elements connected to each other only at the midsurface cannot exactly describe the true displacements, strains and stresses in the vicinity of the interface between two elements, where discontinuities in the material properties occur. This is clearly manifested by the discontinuous slope of rotation ϕ_r in Fig. 7(b). It is reasonable to assume that the detailed modeling of the interface between two elements made of dissimilar materials bears analogy to the modeling of the boundary layer at truly clamped plate edges [e.g. $U_r(a, z) \equiv U_z(a, z) \equiv 0$], which requires the use of Papkovich–Fadle eigenfunctions [16]. In conclusion, the exact interior finite elements essentially extend the applicability of the exact interior elasticity solution to more complicated settings. However, we can also see how conventional midsurface-based modeling and the lack of a boundary layer may lead to results that are not necessarily in agreement with full 3D results.

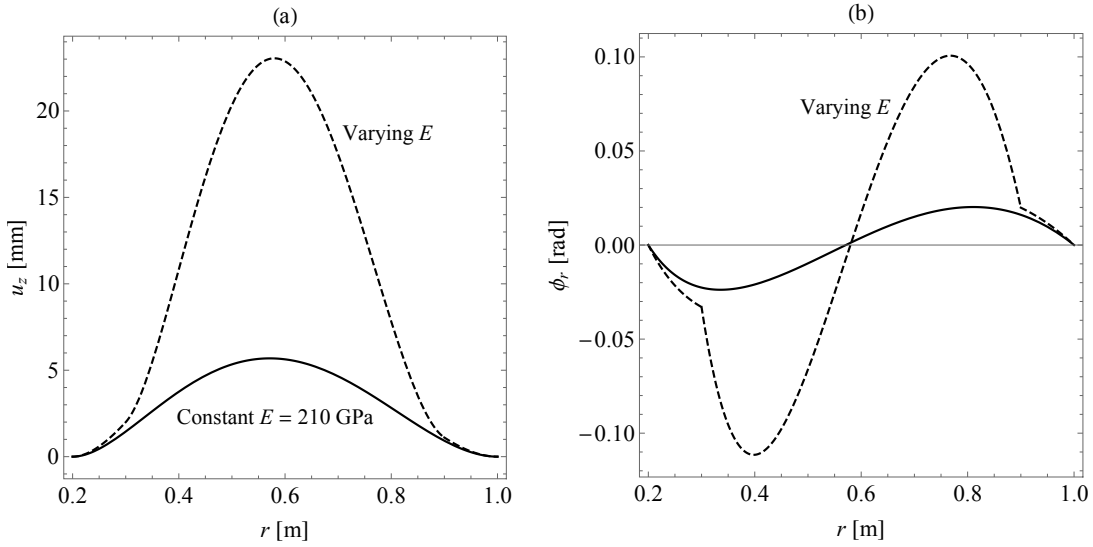

Figure 7: a) Transverse deflection and b) rotation of the normal of the plate shown in Fig. 6 calculated using three exact interior finite elements.

6. Conclusions

In this paper, we formulated an exact finite element for a linearly elastic annular circular plate using a general elasticity solution. The element was developed in an interior bending framework without considering edge effects. In such a framework, the interior stresses act as surface tractions on the lateral plate edges and contribute to the total potential energy of the plate. It is crucial to account for this feature in all energy-based considerations. The developed plate element provides a straightforward way to obtain closed-form axisymmetric interior elasticity solutions to many practical problems. For example, by using two elements for an annular plate, a nodal shear force in the node that the elements share can be used to describe a uniform ring load. In addition to their importance in engineering, the solutions may be used to validate theoretically and computationally more involved finite elements such as isoparametric quadrilateral plate elements.

Acknowledgements

The authors acknowledge the Finland Distinguished Professor (FiDiPro) programme: "Nonlinear response of large, complex thin-walled structures" supported by Tekes (The Finnish Funding Agency for Technology and Innovation) and industrial partners Napa, SSAB, Deltamarin, Konetekknologiakeskus Turku and Meyer Turku.

References

[1] Szilard R. Theories and applications of plate analysis: classical numerical and engineering methods. John Wiley & Sons; 2004.
[2] Reddy JN. Theory and analysis of elastic plates and shells. CRC press; 2006.
[3] Wang CM, Lim GT, Sim CC. Bending solutions of axisymmetric Levinson plates in terms of corresponding Kirchhoff solutions. J Eng Mech–ASCE 2001;127(12):1296–308.
[4] Reddy JN, Wang CM, Lam KY. Unified finite elements based on the classical and shear deformation theories of beams and axisymmetric circular plates. Commun Numer Meth En 1997;13(6):495–510.
[5] Reddy JN, Wang CM. Relationships between classical and shear deformation theories of axisymmetric circular plates. AIAA J 1997;35(12):1862–8.
[6] Karttunen AT, von Hertzen R. Interior formulation of axisymmetric Levinson plate theory. Mech Res Commun 2016;74:34–8.
[7] Timoshenko SP, Goodier JN. Theory of Elasticity. Singapore: McGraw-Hill; 3rd ed.; 1970.
[8] Barber JR. Elasticity. New York: Springer; 3rd ed.; 2010.
[9] Gregory RD. The general form of the three-dimensional elastic field inside an isotropic plate with free faces. J Elast 1992;28(1):1–28.
[10] Wang MZ, Zhao BS. The decomposed form of the three-dimensional elastic plate. Acta Mech 2003;166(1-4):207–16.
[11] Zhao B, Wu D, Wang M. The refined theory and the decomposed theorem of a transversely isotropic elastic plate. Eur J Mech A-Solid 2013;39:243–50.
[12] Cheng S. Elasticity theory of plates and a refined theory. J App Mech 1979;46(3):644–50.
[13] Wang FY. Two-dimensional theories deduced from three-dimensional theory for a transversely isotropic body. I: Plate problems. Int J Solids Struct 1990;26(4):455–70.
[14] Wang FY. Two-dimensional theories deduced from three-dimensional theory for a transversely isotropic body. II: Plane problems. Int J Solids Struct 1991;28(2):161–77.
[15] Piltner R. Three-dimensional stress and displacement representations for plate problems. Mech Res Commun 1991;18(1):41–9.
[16] Piltner R. The derivation of a thick and thin plate formulation without ad hoc assumptions. J Elast 1992;29(2):133–73.
[17] Batista M. An exact theory of the bending of transversely inextensible elastic plates. Acta Mech 2015;226(9):2899–924.

[18] Karttunen AT, von Hertzen R. Exact theory for a linearly elastic interior beam. Int J Solids Struct 2016;78:125–30.
[19] Karttunen AT, von Hertzen R. On the foundations of anisotropic interior beam theories. Compos B-Eng 2016;87:299–310.
[20] Vinson JR. Plate and panel structures of isotropic, composite and piezoelectric materials, including sandwich construction. New York: Springer; 2006.
[21] Sadd MH. Elasticity – Theory, Applications and Numerics. Oxford: Academic Press; 3rd ed.; 2014.